

Dissimilar Friction Stir Welding between Magnesium and Aluminum Alloys

Mahdi Salari^{1*}

¹Materials Science and Engineering Dept., Islamic Azad University, Sirjan Branch

*Email of Corresponding Author: msalari@iausrjan.ac.ir

Received: June 28, 2020; Accepted: September 17, 2020

Abstract

Joining two dissimilar metals, specifically Mg and Al alloys, using conventional welding techniques is extraordinarily challenging. Even when these alloys can be joined, the weld is littered with defects such as cracks, cavities, and wormholes. The focus of this study was to use friction stir welding to create a defect-free joint between Al 2139 and Mg WE43. The design included an 11 mm scrolled and concave shoulder in addition to a 6 mm length pin comprised of two tapering, threaded re-entrant flutes that promoted and amplified material flow. Upon completion of this project, an improved experimental setup process was created as well as successful welds between the two alloys. These successful joints, albeit containing defects, lead to the conclusion that the tool used in the project was ill-fit to join the Al and Mg alloy plates. As a result of this aggressive pin design, there was a lack of heat generation towards the bottom of the pin even at higher (800-1000 rpm) rotation speeds. This lack of heat generation prohibited the material from reaching plastic deformation thus preventing the needed material flow to form the defect-free joint.

Keywords

Friction Stir Welding, Al Alloy, Rotation Speed, Mg Alloy

1. Introduction

Across numerous industrial fields, particularly aerospace and automotive, considerable attention has been placed upon aluminum and magnesium alloys due to their high specific strengths and low densities among other unique properties. The primary obstacle with using these alloys is their inability to be joined using traditional fusion or laser welding methods. As a result, these industries are now looking to friction stir welding (FSW) to solve this joining problem. Even with this new founding popularity, there is still little research being conducted on dissimilar FSW of aluminum and magnesium alloys.

Joining two dissimilar metals, specifically Mg and Al alloys, using conventional welding techniques are extraordinarily challenging. Even when they can be joined, the weld is littered with defects such as cracks, cavities, and wormholes. Numerous studies have reported that the use of FSW can be used to join dissimilar Al and Mg alloys [1-5].

The study by Y.S. Sato et al. [6] report that the dissimilar weld between Mg AZ31 and Al 1050 contained a large volume of IMC Al₁₂Mg₁₇ and considerably higher hardness in the weld nugget

compared to that of typical Al-Mg welds. During the joining process of Mg AZ31 and Al 1060, Yan et al [7] indicated that $Al_{12}Mg_{17}$ and Al_3Mg_2 cause the weld to crack along the centerline. Yamamoto et al [8] stated that the formation of IMCs was controlled by diffusion of Al and Mg atoms. Using X-ray diffraction analysis, C.B. Jagadeesha [9] also reports the presence of IMCs $Al_{12}Mg_{17}$ and Al_3Mg_2 in the weld volume. The study by Khodir et al [10] reported that in the dissimilar joining of Al 2024 to Mg AZ3 the hardness value varied in the nugget due to the formation of IMCs as the result of constitutional liquation during welding. In this study, dissimilar FSW between Al 2139 and Mg WE43 alloy plates was performed. The goals of this project were to create a defect-free weld and then experimentally investigate the impact of tool rotation speed and offset on the surface appearance of the joined plates.

2. Material and methods

2.1 Base materials

The materials used for butt joints were Mg WE43 and Al 2139 alloy plates. Magnesium Elektron WE43, one of the two alloys being joined in this project, is a high strength casting alloy typically used in power systems, aerospace engines, and missiles [11]. This is due to WE43's high tensile strength of 250 MPa and a low density of 1.8 g/cm^3 . With a melting temperature of $540\text{-}640^\circ\text{C}$, it can withstand operating temperatures of up to 300°C [11]. WE43 is also highly sought after because of the alloy's excellent corrosion resistance. The chemical composition of Mg WE43 was: 4% Y, 0.4% Zr, and 95% Mg.

Dimensions for the Mg alloy plates used in this study are 6 inches high, 2 inches wide, and $7/16$ of an inch thick. See Table 1 for the chemical composition of Mg WE43. Aluminum 2139, the alloy being joined to Mg WE43, is a recently created alloy that is being implemented across several high profile entities [12]. With a density of 2.81 g/cm^3 , the maximum yield stress of 51 ksi, and maximum ultimate stress of 60 ksi, Al 2139 is an ideal alloy in both aerospace and ground vehicles [12]. Chemical composition of Al 2139 was: 5% Cu, 0.6% Mn, 0.5% Ag, 0.4% Mg and 93% Al. Dimensions for the Al alloy plate are 6 inches in height, 4 inches wide, and 7.2 of an inch thick [13-16].

2.2 Welding parameters

The stir tool, made of H13 tool steel, is of fixed design. The design includes an 11 mm diameter shoulder which is scrolled and concave to best generate heat while ensuring the material does not escape during the joining process. The tool also contains a 6 mm length pin. The pin is comprised of two tapering, threaded re-entrant flutes that promote and amplify the material flow. The tilt was set to 5° and remained so until the end of the project. Due to the tool's fixed design and length, an ideal plunge depth was quickly determined to be 6.05 mm. This depth allowed for complete shoulder contact with the surface of the plates while not plowing through the material. The plunge speed was set to 1 mm s^{-1} . At this speed, the plates were able to maintain contact throughout the initial plunging process. The best results were observed with a .35 mm offset. This is not to say this is the ideal offset. Since the previous runs were inconclusive, upon the return of the repaired table, the project was resumed setting the rotation speed at 1000 RPM.

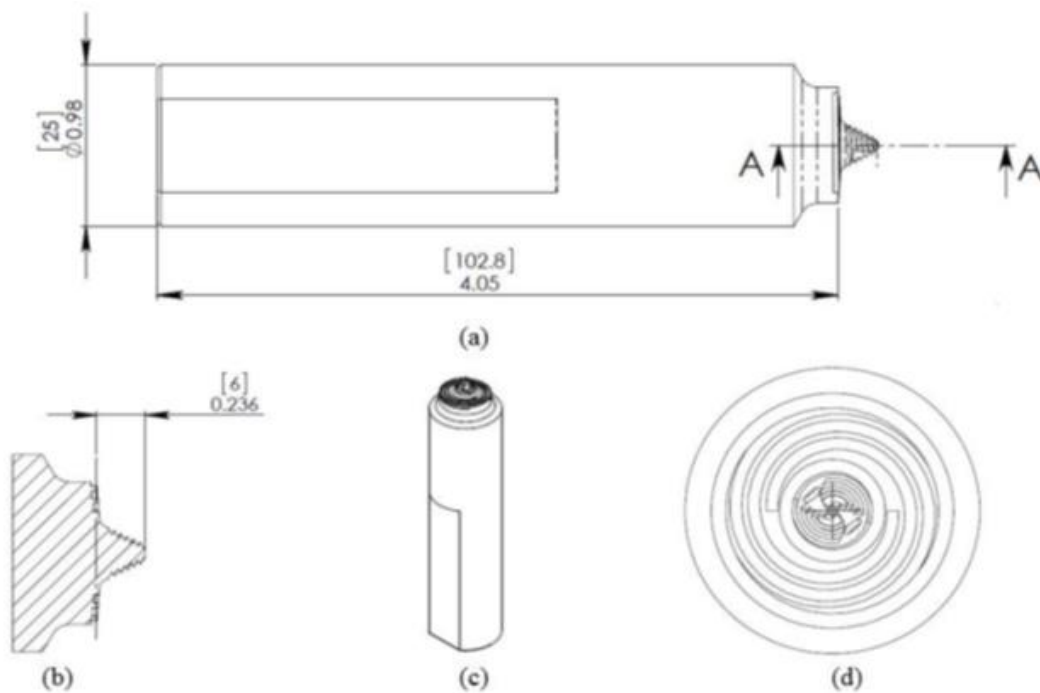


Figure 1. (a) Tool length of 102.8 mm; (b) Pin length of 6 mm; (c) Fixed tool design; (d) Scrolled shoulder with two flutes

3. Results and discussion

It was observed that the surface of the plates, more so Mg than Al, had melted during the FSW process. This was due to the high rotation speed coupled with the scrolled shoulder. Since melting, or fusing, the two alloys together was not the objective of this project, the rotation speed had to be decreased. By diminishing the rotation speed by 50 rpm each run, the melting problem was solved and better mixing was achieved. It wasn't until the rotation speed reached 350 rpm that improvements stop occurring.

As seen in Figure 2, at 400 RPM there was minimal melting, the gap between the two plates was one of the smallest, and the magnesium appeared to be mixed within the stir zone better than all the previous runs. Furthermore, there was a loud "popping" sound heard immediately following the completion of the FSW process. This noise is believed to be the result of the IM layer being created along the joint line. An IM (Inter Metallic) layer, may briefly be described as "solid phases containing two or more metallic elements with optionally one or more non-metallic elements, whose crystal structure differs from that of the other constituents".

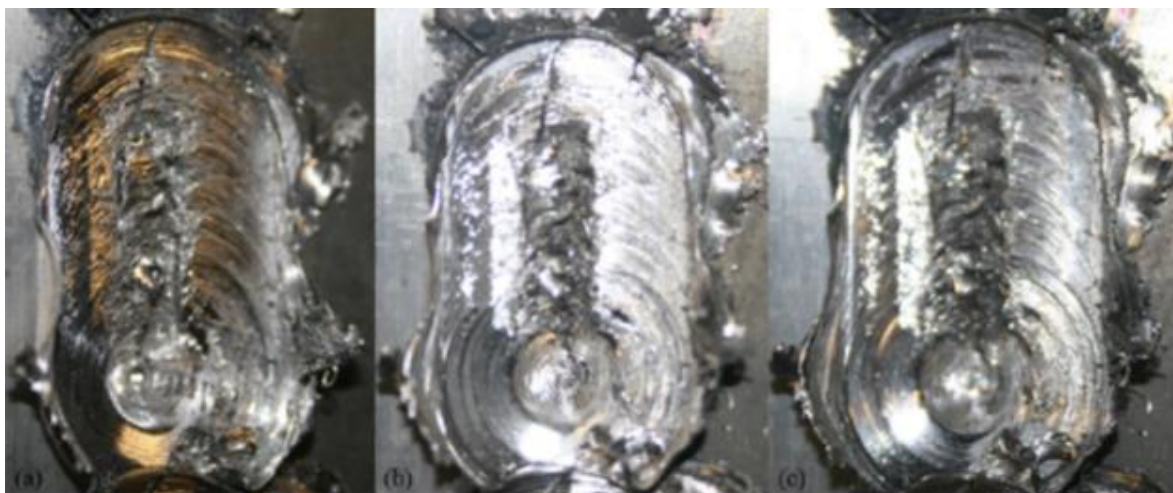


Figure 2. Weld at 400 rpm; (a), (b), and (c) represent different camera focal points

To better understand the surface effects and crack propagation due to varying tool rotation speeds, welded samples were observed utilizing an optical microscope. The tool rotation speeds that were analyzed were 500, 450, 400, and 350 rpm. Both the Mg and Al side of each weld was studied as well as each crack along the joint line. When observing the 500 rpm weld with the naked eye, it was noted that the Mg side of the weld contained a metallic and smooth surface. This was predominately due to the excess heat generated by the scrolled shoulder used in this project and the tool being offset to the Mg side.

Figure 3 depicts the Mg side of the 500 rpm weld where excess heat generation occurred. When comparing the Mg side of the weld (Figure 3c) to the Al side (Figure 3a), there is a noticeable difference in each flow pattern. On the Al side, the flow pattern is clearly defined and is consistent throughout the weld which reflects previous successful welds with other materials in the lab at UNT in addition to published literature [11].

On the Mg side, the flow pattern is difficult to discern as a result of the Mg surface melting during the joining process. If FSW is to create a defect-free weld with minimal IMCs, the two materials cannot exceed their respective melting temperatures while being joined. Contrary to published data, the crack between the two alloy plates did not follow the IM layer as seen in Figure 3b.

The major crack follows the joint line through the Al side only which leads us to believe it was a result of mechanical failure during the process. Meaning that the two plates were not securely held together during the joining process and also due to the lack of material flow from one side to the other thus not filling the SZ. The large crack could also be caused by residual stress left behind by the built-up downward pressure caused by the FSW machine. Even with these issues, the 500 rpm tool rotation speed created one of the smallest cracks with an average size of 0.28 mm.

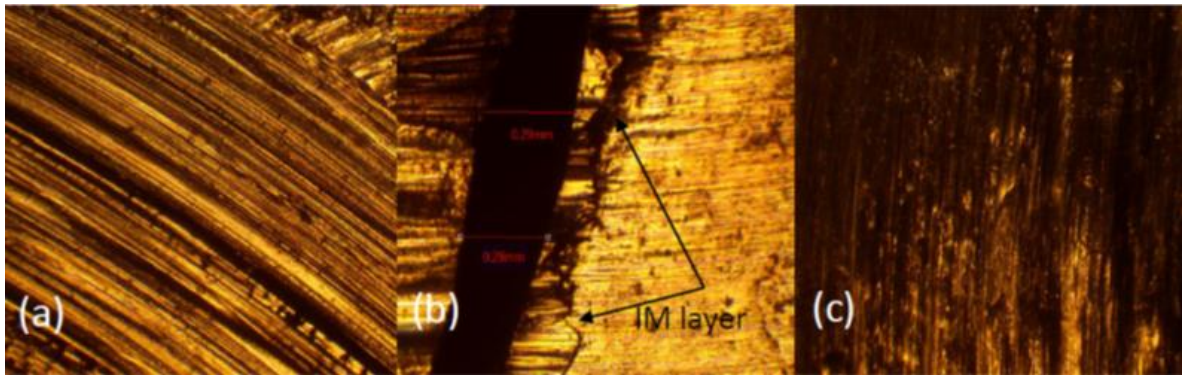


Figure 3. Rotational speed of 500 rpm: (a) Al side of the weld; (b) 0.28 mm crack in SZ; (c) Mg side of the weld

Similar to the 500 rpm experiment, the weld created using a tool rotation speed of 450 rpm still generated too much heat on the surface of the Mg side. This is illustrated by the lack of a well-defined flow pattern on the Mg side (Figure 4a) as well as a metallic and smooth surface. When compared to that of the Al side (Figure 4c), there appears to be less cracking which might seem to be a positive result, but this is not the case. There are small cracks and fissures along the Al side which are side effects of the large crack being formed. It is worth noting that by reducing the tool rotation speed from 500 to 450 RPM there was flow improvement on the Mg side. Although the crack width increased to an average of 0.6 mm (Figure 4b), this is not a clear indication that the tool rotation speed parameter was moving in the wrong direction. Note that the major crack still formed only on the Al side of the weld and not along with the IM layer. This tells us that the crack was not a product of IMCs, $Al_{12}Mg_{17}$ for example, being formed in the SZ.

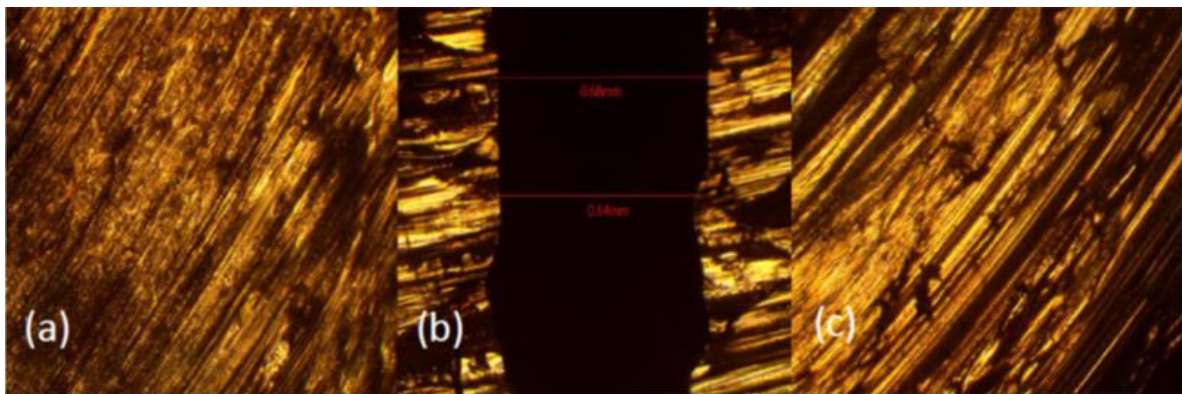


Figure 4. Rotational speed of 450 rpm: (a) Mg side of the weld; (b) 0.66 mm crack in SZ; (c) Al side of the weld

Reducing the tool rotation speed by another 50 rpm yielded additional material flow and reduced heat generation on the Mg side of the weld as seen in Figure 5a. A clear material flow pattern, although not as defined as the Al side (Figure 5c), can be seen which is a clear sign that lower rotation speeds is where this project's tool should be operated at the lack of material flow from the front to the back of the tool's pin still caused a large crack to form as seen in Figure 5b. If a defect-free weld is to be created between Al 2139 and Mg WE43 alloys, this issue must be addressed and resolved.

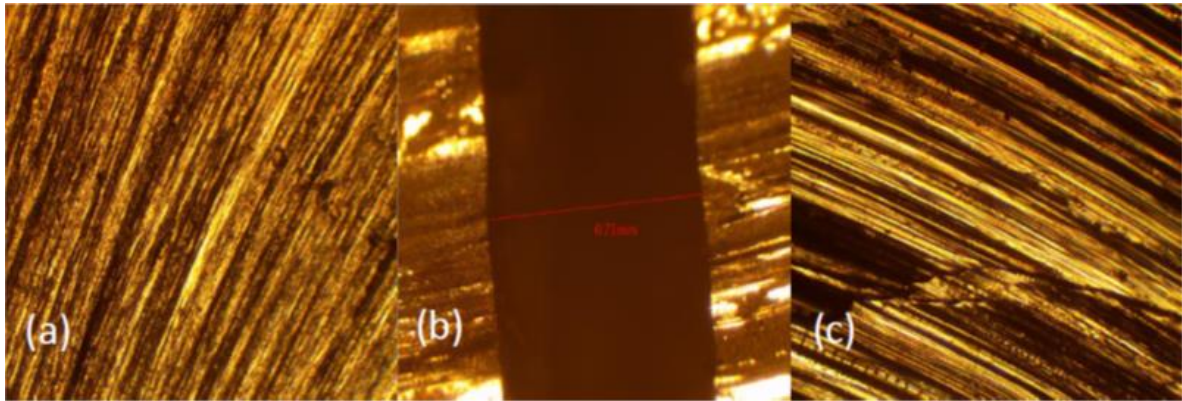


Figure 5. Rotational speed of 400 rpm: (a) Mg side of the weld; (b) 0.71 mm crack in SZ; (c) Al side of the weld

As seen in Figure 6a, particularly in the lower right-hand corner, the material flow on the Mg side of the weld increased yet again when reducing the tool rotation speed by 50 rpm. Flow on the Al side remained well defined at a tool rotation speed of 350 rpm (Figure 6c). The crack's average width came to be 0.37 mm as seen in Figure 6b. These images further confirmed that the optimal tool rotation speed below 500 rpm.

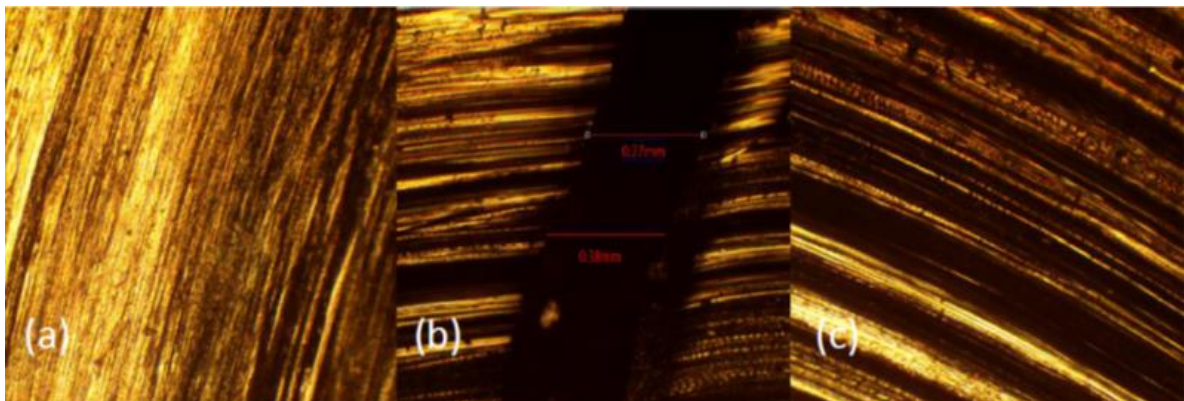


Figure 6. Rotational speed of 350 rpm: (a) Mg side of the weld; (b) 0.37 mm crack in SZ; (c) Al side of the weld

4. Conclusion

Upon completion of this project, an improved experimental setup process was created as well as successful welds between Al 2139 and Mg WE43 alloy plates. These successful joints, albeit containing defects, and the data that accompanied them provided essential information that would eventually lead students in the lab to a better understanding of dissimilar FSW. Accompanying this enlightenment came the conclusion that the dual-flute and scrolled shoulder tool used in this project was ill-fit to join the Al and Mg alloy plates. This was primarily due to its conical shaped pin. As a result of this “aggressive” pin design, there was a lack of heat generation towards the bottom of the pin even at higher (800-1000 rpm) rotation speeds. This lack of heat generation prohibited the material from reaching plastic deformation thus causing the material to be shredded and deposit debris in the SZ.

5. References

- [1] Sameer, M. and Anil Kumar, B. 2019. Mechanical and metallurgical properties of friction stir welded dissimilar joints of AZ91 magnesium alloy and AA 6082-T6 aluminium alloy. *Journal of Magnesium and Alloys*. 7: 264-271.
- [2] Rajendran, C. and Srinivasan, K. 2019. Effect of tool tilt angle on strength and microstructural characteristics of friction stir welded lap joints of AA2014-T6 aluminum alloy. *Transactions of Nonferrous Metals Society of China*. 29: 1824-1835.
- [3] Peiqi, L., Guoqiang, Y., Hengyu, W. and Sha, L. 2019. Friction stir welding between the high-pressure die casting of AZ91 magnesium alloy and A383 aluminum alloy. *Journal of Materials Processing Technology*. 264: 55-63.
- [4] Boccarusso, L., Astarita, A. and Carlone, P. 2019. Dissimilar friction stir lap welding of AA 6082 - Mg AZ31: Force analysis and microstructure evolution. *Journal of Manufacturing Processes*. 44: 376-388.
- [5] Jedrasiak, P. and Shercliff, H. 2019. Small strain finite element modelling of friction stir spot welding of Al and Mg alloys. *Journal of Materials Processing Technology*. 263: 207-222.
- [6] Sato, Y., Park, S. and Kokawa, H. 2001. Microstructural factors governing hardness in friction-stir welds of solid-solution-hardened Al alloys. *Metallic Materials Transactions*. 32:3033–3042.
- [7] Yan, J., Sutton, A. and Reynolds, A. 2005. Process structure property relationships for nugget and heat affected zone regions of AA2524-T351 friction stir welds, *Science and Technology of Welding and Joining*, 10: 725-36.
- [8] Yamamoto, N., Liao, J., Watanabe, S. and Nakata, K. 2009. Effect of intermetallic compound layer on tensile strength of dissimilar friction-stir weld of high strength Mg alloy and Al Alloy. *Materials Transactions*. 50: 2833-2838.
- [9] Jagadeesha, C. 2014. Dissimilar friction stir welding between aluminum alloy and magnesium alloy at a low rotational speed, *Materials Science and Engineering A*. 616: 55-62.
- [10] Shibayanagi, S., Khodir, A. and Toshiya, D. 2007. Microstructure and Mechanical Properties of Friction Stir Welded Dissimilar Aluminum Joints of AA2024-T3 and AA7075-T6, *Materials Transactions*. 48: 1928-1937.
- [11] Magnesium Elektron WE43 Alloy. AZO Materials. <http://www.azom.com/article.aspx?ArticleID=9279>.
- [12] Cho, A., Lisagor, W. and Bales, T. 2007. Development and Processing Improvement of Aerospace Aluminum Alloys - Development of Al-Cu-Mg-Ag Alloy (2139), *NASA/CR*. 27:215-294.
- [13] Das, J., Banik, S., Reddy, S., Sankar, M. and Robi, P. 2019. Review on process parameters effect on fatigue crack growth rate in friction stir welding. *Materials today processing*. 18: 3061-3070.
- [14] Guangyu, L., Wenming, J., Feng, G., Junwen, Z. and Zitian, F. 2021, Microstructure, mechanical properties and corrosion resistance of A356 aluminum/AZ91D magnesium bimetal prepared by a compound casting combined with a novel Ni-Cu composite interlayer. *Journal of Materials Processing Technology*. 288: 116-128.

- [15] Chunliang, Y., Chuan, S. and Wu, L. 2020, Modeling the dissimilar material flow and mixing in friction stir welding of aluminum to magnesium alloys. *Journal of Alloys and Compounds*. 843:156-162.
- [16] Raval, S. and Judal, K. 2020. Recent Advances in Dissimilar Friction Stir Welding of Aluminum to Magnesium Alloys. *Materials today processing*. 22: 2665-2675.